Electroviscous Effect of Moderately Concentrated Colloidal Suspensions under Overlapping Conditions

Emilio Ruiz-Reina,[†,*] Pablo García-Sánchez,[‡] and Felix Carrique[§]

Departamento de Física Aplicada II, Universidad de Málaga, Campus de El Ejido, 29071 Málaga, Spain, Departamento de Electrónica y Electromagnetismo, Universidad de Sevilla, Campus de Reina Mercedes, 41012 Sevilla, Spain, and Departamento de Física Aplicada I, Universidad de Málaga, Campus de Teatinos, 29071 Málaga, Spain

Received: November 25, 2004; In Final Form: January 18, 2005

In this work we present a theoretical model for the calculation of the electroviscous coefficient of a colloidal suspension. The treatment is not limited for dilute suspensions and includes the contribution of the overlapping between adjacent ionic layers. The development here used is based on a cell model, which is applicable to Newtonian suspensions under low shear conditions and without crystalline ordering. Also presented are a complete study of the new numerical results and comparisons with previous results. We find new behaviors for the case of moderate volume fractions that do not appear in the dilute limit.

Introduction

The viscosity η of a dilute suspension of spherical, rigid and nonslipping colloidal particles was first calculated by Einstein,[1]

$$\eta = \eta_0\left(1 + \frac{5}{2}\phi\right) \tag{1}$$

where η_0 is the viscosity of the suspending medium and ϕ is the particle volume fraction. The increase in suspension viscosity is due to the distortion of the applied flow field in the neighborhood of the particles. When the particles are charged, there is an additional increment of the flow distortion and, consequently, of the viscosity, which is caused by the presence of electric double layers around the particles. This phenomenon is called the primary electroviscous effect and Einstein's equation is modified to take it into account,

$$\eta = \eta_0\left(1 + \frac{5}{2}\phi(1 + p)\right) \tag{2}$$

where p, the primary electroviscous coefficient, is a function of the charge on the particle and properties of the suspending electrolyte. The thickness of the electric double layer is given by the Debye length κ^{-1},

$$\kappa^2 = \frac{e^2}{\epsilon_0 \epsilon_{rs} k_B T} \sum_{i=1}^{N} n_i^{\infty} z_i^2 \tag{3}$$

where e is the elementary electric charge, k_B is Boltzmann's constant, T is the absolute temperature, ϵ_{rs} is the relative permittivity of the suspending medium, ϵ_0 is the vacuum permittivity, and n_i^{∞} and z_i are the bulk number density and valence of i-type ions.

The primary electroviscous coefficient is of small magnitude and its experimental determination is difficult.[2,3] Most of the experimental works[4−11] on the primary electroviscous effect find that it is underestimated by the theoretical models.[12−17]

Recently, it has been presented various theories that try to predict the experimental results. Rubio-Hernández et al.[18−21] and Sherwood et al.[22] included in the theoretical models the contribution of the ionic transport into the Stern layer. They found an improvement of the predictions when the influence of a dynamic Stern layer was taken into account in both the viscosity calculations and experimental determinations of the state of charge and properties of the suspension. Their conclusion was that it is necessary to consider the presence of a Stern layer in the complete experimental study of the suspension in a consistent form. García-Salinas and de las Nieves[3] studied the influence of the reduction of ionic diffusion in the neighborhood of the colloidal particles and found a better theory-experiment agreement.

If the suspension of charged particles cannot be considered dilute, we distinguish three cases:

(1) *The electrical double layer thickness is larger than the interparticle distance*. In this case the electrical interactions (i.e., the stresses arising from the very high overlapping of electrical double layers and the strong alteration of collision trajectories) are considerably greater than the stresses due to hydrodynamic interactions. The suspension forms a colloidal crystal and its flow behavior is extremely shear-thinning, being very difficult to find experimentally a low-shear viscosity "plateau". Our theory is, obviously, not applicable in this case.

(2) *The electrical double layer thickness is comparable with the interparticle distance.* In this case there is a low overlapping of electrical double layers, in addition to the hydrodynamic interactions. The suspension does not present crystalline ordering because the electrical interactions, although great enough to noticeably contribute to the viscosity of the suspension, are not sufficiently high.

(3) *The electrical double layer thickness is quite smaller than the interparticle distance*. In this case electrical interactions are masked by the hydrodynamic interactions (there is not overlapping of electrical double layers and the modification of collision trajectories is low). The suspension is disordered at rest and

* Corresponding author. E-mail: eruizr@uma.es.
† Universidad de Málaga, Campus de El Ejido.
‡ Universidad de Sevilla.
§ Universidad de Málaga, Campus de Teatinos.

10.1021/jp044619p CCC: $30.25
Published on Web 02/23/2005

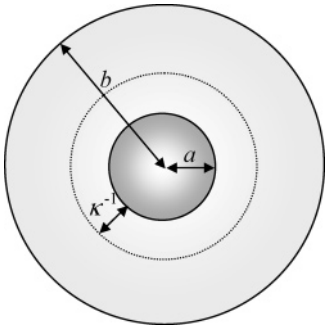

Figure 1. The cell model.

shows a wide low-shear Newtonian "plateau". However, the distortion of the electrical double layer modifies the hydrodynamic interactions, because the flow fields around the particles are different than in the case of uncharged particles.

Ruiz-Reina et al.[2] developed a theoretical model of the electroviscous effect (we eliminate the word "primary" because the suspension has not to be necessarily dilute) that includes the possibility of hydrodynamic interactions and can predict the electroviscous coefficient for suspensions that fit into case 3 described before. The objective of the present work is the modification of that previous model to introduce the overlapping of electrical double layers. In this way, the range of validity of the theory is extended for suspensions in case 2 as well.

Theory

Cell Model. To take into account the hydrodynamic particle−particle interactions, Happel's cell model[23] with Simha's hydrodynamic boundary conditions[24] at the outer surface of the cell will be used.

The cell model concept has been successfully applied to develop theoretical models for different electrokinetic phenomena in moderately concentrated colloidal suspensions of charged particles, such as static electrophoresis and electrical conductivity,[28−31] sedimentation velocity and potential,[32,33] dynamic electrophoresis,[34−36] complex conductivity and dielectric response,[37] and electroacoustic phenomena,[38,39] to mention just a few.

According to this model (Figure 1), each spherical particle of radius a is surrounded by a concentric shell of an electrolyte solution, having an outer radius b such that the particle/cell volume ratio in the cell is equal to the particle volume fraction throughout the entire suspension, i.e.,

$$\phi = \left(\frac{a}{b}\right)^3 \tag{4}$$

The surface $r = a$ is usually called the "slip-plane". This is the plane outside which the continuum equations of hydrodynamics are assumed to hold. In this work we assume that the slip-plane coincides with the true surface of the particle, and that there is not any effect arising from mobile adsorbed ions in the dynamic Stern layer.

The basic assumption of the cell model is that the suspension properties can be derived from the study of a unique cell. The disturbance due to the presence of each solid sphere is considered to be confined inside the cell. According to Simha, each cell enclosing fluid is surrounding by a rigid spherical wall and the perturbations of the different magnitudes disappear at the surface of the cell ($r = b$). By its own nature, the cell model is only applicable when the suspension is homogeneous and isotropic. Therefore, Brownian motion should be dominant over other potential fields to prevent structural ordering of the particles. When a flow field is imposed, this is only true in the low shear region.

Different boundary conditions on the surface of the cell can be found in the literature. Simha's boundary condition[24] arises from his hypothesis of no disturbance velocity at the cell wall, $\mathbf{u}' = 0$. In an alternative treatment, Happel[23] introduced a different hypothesis about the behavior of the disturbances at $r = b$. He assumed that only the normal component of the perturbation velocity vanishes at the surface of the cell, supplemented with the condition of no friction on it due to the disturbance, which corresponds to the vanishing of the tangential components of the stress perturbation.

Simha's boundary conditions[24] for the cell model leads to Einstein's result valid for uncharged particles at the limit condition $\phi \rightarrow 0$. This is not true when Happel's conditions are used. Therefore, we decided to use Simha's instead of the others.

Governing equations. Let us consider now a charged spherical particle of radius a immersed in an electrolyte solution composed by N ionic species of valences z_i, bulk number concentrations n_i^∞, and drag coefficients λ_i ($i = 1, ..., N$). The axes of the spherical coordinate system (r, θ, φ) are fixed at the center of the particle. In the absence of any flow field, the particle is surrounded by a radial charge distribution and a uniform electric potential, the ζ-potential, at $r = a$.

We will consider the case when a flow field is applied to the suspension. If a linear shear field is applied to the system, the velocity field $\mathbf{u}(\mathbf{r})$ can be written as

$$\mathbf{u}(\mathbf{r}) = \alpha\cdot\mathbf{r} + \nabla \times \nabla \times [\alpha\cdot\nabla f(r)] \tag{5}$$

where α is a constant second-order tensor and $f(r)$ is a function that only depends on the radial coordinate. The second term corresponds to the perturbation in the flow field due to the presence of particles in the suspension.[25]

A complete solution of the problem would require the knowledge of the electric potential $\Psi(\mathbf{r})$, the number density $n_i(\mathbf{r})$ and the drift velocity $\mathbf{v}_i(\mathbf{r})$ of each type of ions, the fluid velocity $\mathbf{u}(\mathbf{r})$, and the pressure $P(\mathbf{r})$ at every point $\mathbf{r}$ in the system. The governing equations for these fields are[16]

$$\nabla^2\Psi(\mathbf{r}) = -\frac{\rho_{el}(\mathbf{r})}{\epsilon_{rs}\epsilon_0} \tag{6}$$

$$\rho_{el}(\mathbf{r}) = \sum_{i=1}^{N} z_i e n_i(\mathbf{r}) \tag{7}$$

$$\eta_0\nabla^2\mathbf{u}(\mathrm{r}) - \nabla P(\mathbf{r}) = \rho_{el}(\mathbf{r})\nabla\Psi(\mathbf{r}) \tag{8}$$

$$\nabla\cdot\mathbf{u}(\mathbf{r}) = 0 \tag{9}$$

$$-\lambda_i[\mathbf{v}_i(\mathbf{r}) - \mathbf{u}(\mathbf{r})] - \mathrm{z}_i e\nabla\Psi(\mathbf{r}) - k_B T\nabla \ln n_i(\mathbf{r}) = 0 \qquad i = 1, ..., N \tag{10}$$

$$\nabla\cdot[n_i(\mathbf{r})\mathbf{v}_i(\mathbf{r})] = 0 \qquad i = 1, ..., N \tag{11}$$

Equation 6 is Poisson's equation, where $\rho_{el}(\mathbf{r})$ is the electric charge density given by eq 7. Equations 8 and 9 are the Navier−Stokes equations appropriate to a steady incompressible fluid flow at low Reynolds number in the presence of an electrical body force. Equation 10 expresses the balance of hydrodynamic drag, where λ_i are the drag coefficients, electrostatic and thermodynamic forces on ions of type i at position $\mathbf{r}$. Finally, eq 11 is the continuity equation of the number of type-i ions.

For a low shear field, represented by a symmetric (only the symmetric part of the velocity gradient tensor contributes to dissipation of energy and, consequently, to the viscosity of the suspension) and traceless (because the liquid medium is incompressible) tensor α, the following perturbation scheme applies,

$$n_i(\mathbf{r}) = n_i^0(r) + \delta n_i(\mathbf{r}) \qquad i = 1, ..., N \tag{12}$$

$$\Psi(\mathbf{r}) = \Psi^0(r) + \delta\Psi(\mathbf{r}) \tag{13}$$

$$\rho_{el}(\mathbf{r}) = \rho_{el}^0(r) + \delta\rho_{el}(\mathbf{r}) \tag{14}$$

where $\delta n_i(\mathbf{r})$, $\delta\Psi(\mathbf{r})$, and $\delta\rho_{el}(\mathbf{r})$ are the perturbation terms. The equilibrium quantities (with superscript 0) are related by

$$n_i^0(r) = n_i^\infty \exp\left[-\frac{z_i e \Psi^0(r)}{k_B T}\right] \qquad i = 1, ..., N \tag{15}$$

$$\frac{1}{r^2}\frac{d}{dr}\left(r^2\frac{d\Psi^0(r)}{dr}\right) = -\frac{\rho_{el}^0(r)}{\epsilon_{rs}\epsilon_0} \tag{16}$$

$$\rho_{el}^0(r) = \sum_{i=1}^{N} z_i e n_i^0(r) \tag{17}$$

The imposed linear shear field is low and the distortion of the system from equilibrium is small. It is well-known that the suspension has a Newtonian behavior in this case (linear relationship between the volume-averaged stress and shear rate tensors), as can be seen in typical flow curves.[40] The concentration of ions $n_i(\mathbf{r})$ around the particles will change slightly, and we define the perturbation terms $\Phi_i(\mathbf{r})$ as[16]

$$n_i(\mathbf{r}) = n_i^\infty \exp\left[-\frac{z_i e}{k_B T}\{\Psi(\mathbf{r}) + \Phi_i(\mathbf{r})\}\right] \qquad i = 1, ..., N \tag{18}$$

which allows us to write, in combination with eq 12,

$$\delta n_i(\mathbf{r}) = -\left(\frac{z_i e}{k_B T}\right) n_i^0(r)[\delta\Psi(\mathbf{r}) + \Phi_i(\mathbf{r})] \qquad i = 1, ..., N \tag{19}$$

Making use of the symmetry of the problem, it is possible to separate radial and angular dependences,

$$\delta\Psi(\mathbf{r}) = \psi(r)(\hat{\mathbf{r}}\cdot\alpha\cdot\hat{\mathbf{r}}) \tag{20}$$

$$\Phi_i(\mathbf{r}) = \phi_i(r)(\hat{\mathbf{r}}\cdot\alpha\cdot\hat{\mathbf{r}}) \qquad i = 1, ..., N \tag{21}$$

where $\hat{\mathbf{r}}$ is the unitary vector ($\hat{\mathbf{r}} = \mathbf{r}/r$, r being the modulus of the position vector $\mathbf{r}$).

Substituting eqs 12−19 into the differential eqs 6−11, neglecting products of small perturbation quantities, and applying the symmetry eqs 5, 20, and 21 transform the governing equations into

$$L_4F(r) = -\frac{2e^2}{r^2\eta_0 k_B T}\left(\frac{d\Psi^0}{dr}\right)\sum_{i=1}^{N} n_i^0(r) z_i^2 \phi_i(r) \tag{22}$$

$$L_2\phi_i(r) = \frac{e z_i}{k_B T}\left(\frac{d\Psi^0}{dr}\right)\left[\frac{d\phi_i}{dr} + \frac{\lambda_i}{z_i e}\{r - 3F(r)\}\right] \qquad i = 1, ..., N \tag{23}$$

$$L_2\psi(r) - \frac{1}{\epsilon_{rs}\epsilon_0 k_B T}\sum_{i=1}^{N} z_i^2 e^2 n_i^0(r)[\psi(r) + \phi_i(r)] = 0 \tag{24}$$

The function $F(r)$ is defined by

$$F(r) = \frac{d}{dr}\left(\frac{1}{r}\frac{df(r)}{dr}\right) \tag{25}$$

and the differential operators L_2 in eqs 23 and 24 and L_4 in eq 22 are defined by

$$L_2\psi \equiv \frac{d^2\psi}{dr^2} + \frac{2}{r}\frac{d\psi}{dr} - \frac{6\psi}{r^2} \tag{26}$$

$$L_4F \equiv \frac{d^4F}{dr^4} + \frac{8}{r}\frac{d^3F}{dr^3} - \frac{24}{r^3}\frac{dF}{dr} + \frac{24}{r^4}F \tag{27}$$

The $N + 2$ coupled differential eqs 22−24 must be solved with specific boundary conditions. The boundary conditions used here are

$$\Psi^0(a) = \zeta \quad \text{(a)} \qquad \text{or} \qquad \left.\frac{d\Psi^0}{dr}\right|_{r=a} = -\frac{\sigma}{\epsilon_{rs}\epsilon_0} \quad \text{(b)} \tag{28}$$

$$\left.\frac{d\Psi^0}{dr}\right|_{r=b} = 0 \tag{29}$$

$$\mathbf{u}(\mathbf{r})|_{r=a} = 0 \tag{30}$$

$$\mathbf{u}(\mathbf{r})|_{r=b} = \alpha\cdot\mathbf{r} \tag{31}$$

$$n_i(\mathbf{r})|_{r=b} = n_i^0(b) \qquad i = 1, ..., N \tag{32}$$

$$\hat{\mathbf{r}}\cdot\mathbf{v}_i(\mathbf{r})|_{r=a} = 0 \Rightarrow \hat{\mathbf{r}}\cdot\nabla\Phi_i(\mathbf{r})|_{r=a} = 0 \tag{33}$$

$$\delta\Psi(\mathbf{r})|_{r=a} = \delta\Psi_p(\mathbf{r})|_{r=a} \tag{34}$$

$$\epsilon_{rs}(\nabla\delta\Psi(\mathbf{r})\cdot\hat{\mathbf{r}})|_{r=a} = \epsilon_{rp}(\nabla\delta\Psi_p(\mathbf{r})\cdot\hat{\mathbf{r}})|_{r=a} \tag{35}$$

$$\nabla\delta\Psi\cdot\hat{\mathbf{r}}|_{r=b} = 0 \tag{36}$$

where $\Psi_p(\mathbf{r})$ is the electric potential inside the particle and ϵ_{rp} is its relative permittivity.

The electric state of the particle surface can be specified by condition (28a), which introduces the ζ-potential in the usual way, or by condition (28b), where σ is the surface charge density. The condition (29) implies that the cell is electrically neutral as a whole. Equation 30 reflects the no slip-condition at the surface of the particle. The condition (31) is that by Simha,[24] which considers that the perturbation of the dilatational flow $\nabla \times \nabla \times (\alpha\cdot\nabla f(r))$ is zero at $r = b$. The condition (32) expresses that the alteration of the equilibrium ion distribution disappears on the cell boundary. Equation 33 arises from the impenetrability of the particle surface by the ions. Equation 34 comes from the continuity condition for the electric potential at the particle surface. Expression (35) follows from the discontinuity of the normal component of the electric displacement vector. Finally, eq 36 ensures that the electroneutrality of the cell is maintained when the flow field is imposed.

According to the symmetry eqs 5, 20, and 21, the boundary conditions given by eqs 30−36 transform into

$$F(a) = \frac{a}{3} \qquad \left.\frac{dF}{dr}\right|_{r=a} = \frac{1}{3} \tag{37}$$

$$F(b) = 0 \qquad \left.\frac{dF}{dr}\right|_{r=b} = 0 \tag{38}$$

$$\phi_i(b) = -\psi(b) \qquad i = 1, ..., N \tag{39}$$

$$\left.\frac{d\psi}{dr}\right|_{r=b} = 0 \tag{40}$$

$$\left.\frac{d\phi_i}{dr}\right|_{r=a} = 0 \qquad i = 1, ..., N \tag{41}$$

$$\left.\frac{d\psi}{dr}\right|_{r=a} - \frac{2\epsilon_{rp}}{\epsilon_{rs}a}\psi(a) = 0 \tag{42}$$

The derivation of the last condition (42) is not straightforward and is detailed in Appendix 1.

Solving the Equations. To solve the coupled eqs 22−24 with the boundary conditions (37)−(42), the method by DeLacey and White[26] has been used.

The far field asymptotic behavior $r \rightarrow b$ of the differential equations system, using condition (29), is

$$L_4F(r) \approx 0 \tag{43}$$

$$L_2\chi(r) - A\chi(r) \approx 0 \tag{44}$$

where we have defined the $N + 1$ column vector $\chi(r)$ and the $(N + 1) \times (N + 1)$ matrix $\mathbf{A}$ as

$$\chi(r) = \begin{pmatrix} \phi_1 \\ \cdots \\ \phi_N \\ \psi \end{pmatrix} \qquad \mathbf{A} = \begin{pmatrix} 0 & 0 & \cdots & 0 & 0 \\ 0 & 0 & \cdots & 0 & 0 \\ \cdots & \cdots & \cdots & \cdots & \cdots \\ 0 & 0 & \cdots & 0 & 0 \\ \beta_1^0 & \beta_2^0 & \cdots & \beta_N^0 & \sum_{i=1}^{N}\beta_i^0 \end{pmatrix}$$

with

$$\beta_i^0 = \frac{z_i^2 e^2 n_i^0(b)}{\epsilon_{rs}\epsilon_0 k_B T} \tag{45}$$

We introduce a new $N + 1$ column vector $X(r) = (X_j)$, $j = 1, ..., N + 1$, such that $X(r) = \mathbf{R}^{-1}\cdot\chi(r)$, where $\mathbf{R}$ is a matrix that diagonalizes $\mathbf{A}$

$$\mathbf{R}^{-1}\cdot\mathbf{A}\cdot\mathbf{R} = \mathrm{diag}(\alpha_1, \alpha_2, ..., \alpha_{N+1}) \tag{46}$$

It can be shown that the eigenvalues α_j are

$$\alpha_j = 0 \qquad (j = 1, ..., N) \qquad \alpha_{N+1} = \sum_{i=1}^{N}\beta_i^0 \tag{47}$$

We finally obtain

$$L_2\mathbf{X} - \mathrm{diag}(\alpha_1, \alpha_2, ..., \alpha_{N+1})\mathbf{X} \approx 0 \tag{48}$$

and for the components of $\mathbf{X}$, the latter becomes

$$L_2X_j - \alpha_jX_j \approx 0 \qquad (j = 1, ..., N + 1) \tag{49}$$

with the solution for $j = 1, ..., N$

$$X_j(r) = A_{j1}S_{j1}(r) + A_{j2}S_{j2}(r) \tag{50}$$

and for $j = N + 1$

$$X_{N+1}(r) = A_{N+1,1}S_{N+1,1}(r) + A_{N+1,2}S_{N+1,2}(r) \tag{51}$$

where

$$S_{j1}(r) = \frac{1}{r^3} \qquad S_{j2}(r) = r^2 \qquad (j = 1, ..., N) \tag{52}$$

$$S_{N+1,1}(r) = \left(\frac{1}{r^3} + \frac{\alpha_{N+1}}{3\,r} + \frac{\sqrt{\alpha_{N+1}}}{r^2}\right) e^{-(\alpha_{N+1})^{1/2}(r-a)} \tag{53}$$

$$S_{N+1,2}(r) = \left(\frac{1}{r^3} + \frac{\alpha_{N+1}}{3\,r} - \frac{\sqrt{\alpha_{N+1}}}{r^2}\right) e^{(\alpha_{N+1})^{1/2}(r-a)} \tag{54}$$

and then

$$\begin{pmatrix} \phi_1(r) \\ \cdots \\ \phi_N(r) \\ \psi(r) \end{pmatrix} = \begin{pmatrix} R_{11} & R_{12} & \cdots & R_{1,N} & R_{1,N+1} \\ R_{21} & R_{22} & \cdots & R_{2,N} & R_{2,N+1} \\ \cdots & \cdots & \cdots & \cdots & \cdots \\ R_{N,1} & R_{N,2} & \cdots & R_{N,N} & R_{N,N+1} \\ R_{N+1,1} & R_{N+1,2} & \cdots & R_{N+1,N} & R_{N+1,N+1} \end{pmatrix} \cdot \begin{pmatrix} A_{11}S_{11}(r) + A_{12}S_{12}(r) \\ A_{21}S_{21}(r) + A_{22}S_{22}(r) \\ \cdots \\ A_{N,1}S_{N,1}(r) + A_{N,2}S_{N,2}(r) \\ A_{N+1,1}S_{N+1,1}(r) + A_{N+1,2}S_{N+1,2}(r) \end{pmatrix} \tag{55}$$

The asymptotic solution for the $F(r)$ function is given by

$$F(r) = \frac{B_1}{r^2} + \frac{B_2}{r^4} + B_3r + B_4r^3 \tag{56}$$

Using the above-mentioned boundary conditions (39) and (40) at $r = b$ with the asymptotic functions, the number of constants can be reduced

$$\phi_i(b) = \sum_{k=1}^{N+1} R_{ik}[A_{k1}S_{k1}(b) + A_{k2}S_{k2}(b)] = - \sum_{k=1}^{N+1} R_{N+1,k}[A_{k1}S_{k1}(b) + A_{k2}S_{k2}(b)] = -\psi(b) \tag{57}$$

$$\frac{d\psi}{dr}(b) = \sum_{k=1}^{N+1} R_{N+1,k}\left[A_{k1}\frac{dS_{k1}}{dr}(b) + A_{k2}\frac{dS_{k2}}{dr}(b)\right] = 0 \tag{58}$$

The A_{k2} constants can be written as a function of the A_{k1} constants and $\psi(b) = -\gamma$, for each k value:

$$\gamma = \frac{b}{2}\left\{ - \frac{5}{b^4}\sum_{j=1}^{N} R_{N+1,j}A_{j1} + A_{N+1,1}\left[\frac{dS_{N+1,1}}{dr}(b) - \frac{S_{N+1,1}(b)}{S_{N+1,2}(b)}\frac{dS_{N+1,2}}{dr}(b)\right]\right\} \tag{59}$$

$$A_{k2} = \frac{\gamma - A_{k1}S_{k1}(b)}{S_{k2}(b)} \qquad k = 1, ..., N \tag{60}$$

$$A_{N+1,2} = -\frac{S_{N+1,1}(b)}{S_{N+1,2}(b)}A_{N+1,1} \tag{61}$$

where the matrix **R** has been chosen to be

$$\mathbf{R} = \begin{pmatrix} 1 & 0 & \cdots & 0 & 0 \\ 0 & 1 & \cdots & 0 & 0 \\ \cdots & \cdots & \cdots & \cdots & \cdots \\ 0 & 0 & \cdots & 1 & 0 \\ -\dfrac{\beta_1^{\,0}}{\sum_{i=1}^{N}\beta_i^{\,0}} & -\dfrac{\beta_2^{\,0}}{\sum_{i=1}^{N}\beta_i^{\,0}} & \cdots & -\dfrac{\beta_N^{\,0}}{\sum_{i=1}^{N}\beta_i^{\,0}} & 1 \end{pmatrix} \tag{62}$$

Substituting the latter result into the asymptotic forms of ϕ_i and ψ yield

$$\begin{pmatrix} \phi_1(r) \\ \cdots \\ \phi_N(r) \\ \psi(r) \end{pmatrix} = \begin{pmatrix} R_{11} & \cdots & R_{1,N+1} \\ \cdots & \cdots & \cdots \\ R_{N+1,1} & \cdots & R_{N+1,N+1} \end{pmatrix} \cdot \begin{pmatrix} A_{11}\left[S_{11}(r) - \dfrac{S_{11}(b)}{S_{12}(b)}S_{12}(r)\right] + \dfrac{\gamma}{S_{12}(b)}S_{12}(r) \\ A_{21}\left[S_{21}(r) - \dfrac{S_{21}(b)}{S_{22}(b)}S_{22}(r)\right] + \dfrac{\gamma}{S_{22}(b)}S_{22}(r) \\ \cdots \\ A_{N+1,1}\left[S_{N+1,1}(r) - \dfrac{S_{N+1,1}(b)}{S_{N+1,2}(b)}S_{N+1,2}(r)\right] \end{pmatrix} \tag{63}$$

As regards the asymptotic function $F(r)$, from boundary condition (38) it becomes

$$F(r) = B_1\left[\frac{1}{r^2} - \frac{5r}{2b^3} + \frac{3r^3}{2b^5}\right] + B_2\left[\frac{1}{r^4} - \frac{7r}{2b^5} + \frac{5r^3}{2b^7}\right] \tag{64}$$

Now, renaming the constants transforms eq 63 into

$$\begin{pmatrix} \phi_1(r) \\ \cdots \\ \phi_N(r) \\ \psi(r) \end{pmatrix} = \begin{pmatrix} R_{11} & \cdots & R_{1,N+1} \\ \cdots & \cdots & \cdots \\ R_{N+1,1} & \cdots & R_{N+1,N+1} \end{pmatrix} \cdot \begin{pmatrix} C_1\left[S_{11}(r) - \dfrac{S_{11}(b)}{S_{12}(b)}S_{12}(r)\right] + \dfrac{\gamma}{S_{12}(b)}S_{12}(r) \\ C_2\left[S_{21}(r) - \dfrac{S_{21}(b)}{S_{22}(b)}S_{22}(r)\right] + \dfrac{\gamma}{S_{22}(b)}S_{22}(r) \\ \cdots \\ C_{N+1}\left[S_{N\,1,1}(r) - \dfrac{S_{N+1,1}(b)}{S_{N+1,2}(b)}S_{N+1,2}(r)\right] \end{pmatrix} \tag{65}$$

and

$$F(r) = C_{N+2}\left[\frac{1}{r^2} - \frac{5r}{2b^3} + \frac{3r^3}{2b^5}\right] + C_{N+3}\left[\frac{1}{r^4} - \frac{7r}{2b^5} + \frac{5r^3}{2b^7}\right] \tag{66}$$

Solutions (65) and (66) are asymptotic, and the $N + 3$ constants C_i will be determined after numerically solving the full system of differential equations and imposing the general solutions to satisfy the boundary conditions given by eqs 37, 41, and 42 at the particle surface.

Effective Viscosity. We will follow a formalism similar to that derived by Batchelor[27] for dilute suspensions of uncharged spheres. However, in our case, use will be made of a cell model to calculate the viscosity of a moderately concentrated suspension. Hydrodynamic interactions between particles will be taken into account by means of Simha's hydrodynamic boundary conditions at the outer surface of the cell.[24] Let the velocity flow field and pressure for a pure straining motion (represented by a symmetrical and traceless tensor α) in the liquid medium be

$$\begin{aligned} u_i &= \alpha_{ij}x_j + u_i' = u_i^{\,0} + u_i' \\ P &= P^0 + P' \end{aligned} \tag{67}$$

where i, j are Cartesian indexes in three dimensions ($i, j = 1-3$) and x_i are the Cartesian coordinates.

The quantities with a prime represent deviations from the corresponding averaged quantities in the suspension (superscript 0). The stress tensor σ_{ij} at any point in the liquid is

$$\sigma_{ij} = -P^0\delta_{ij} + 2\eta_0\alpha_{ij} + \sigma_{ij}' \tag{68}$$

where δ_{ij} is the Kronecker tensor and the additional perturbation stress tensor, σ_{ij}', is defined as

$$\sigma_{ij}' = -P'\delta_{ij} + \eta_0\left(\frac{\partial u_j'}{\partial x_i} + \frac{\partial u_i'}{\partial x_j}\right) \tag{69}$$

The rate at which the forces at the outer surface S of the cell do work is

$$\frac{dW}{dt} = \int_S u_i\sigma_{ik}n_k\,dS = \int_S \alpha_{ij}x_j\sigma_{ik}n_k\,dS = \alpha_{ij}\int_S\left[-P^0\delta_{ik} + 2\eta_0\alpha_{ik} - P'\delta_{ik} + \eta_0\left(\frac{\partial u_{ix}'}{\partial x_k} + \frac{\partial u_k'}{\partial x_i}\right)\right]x_jn_k\,dS \tag{70}$$

n_k ($k = 1-3$) being the coordinates of a unit vector normal to the surface S. In the last expression use has been made of the condition that, at the outer surface of the cell, the perturbation velocity field is zero (just Simha's),

$$u_i' = 0 \Rightarrow u_i = u_i^{\,0} = \alpha_{ij}x_j \tag{71}$$

and then

$$2\alpha_{ij} = \frac{\partial u_i^0}{\partial x_j} + \frac{\partial u_j^0}{\partial x_i} \tag{72}$$

The effective viscosity is defined as that of a homogeneous fluid with the same viscosity of the suspension, η, for which the stress tensor is defined as

$$\sigma_{ij}^* = -P^0\delta_{ij} + 2\eta\alpha_{ij} \tag{73}$$

and the rate of working at the external boundary will be

$$\frac{dW}{dt} = \int_S \alpha_{ij}x_j\sigma_{ik}^*n_k\,dS = \alpha_{ij}\int_S[-P^0\delta_{ik} + 2\eta\alpha_{ik}]x_jn_k\,dS \tag{74}$$

Operating, we obtain

$$\alpha_{ij}\int_S 2\eta\alpha_{ik}x_j n_k \, dS = 2\eta\alpha_{ij}\alpha_{ik}\int_S x_j n_k \, dS = 2\eta\alpha_{ij}\alpha_{ik}\frac{4}{3}\pi b^3\delta_{kj} = 2\eta\alpha_{ij}\alpha_{ij}\frac{4}{3}\pi b^3 \quad (75)$$

Equating the two eqs 70 and 74 representing the energy dissipation rates, the term involving P^0 can be canceled because it is common in both expressions. Taking into account the last eq 75, the dissipation rate equality becomes

$$2\eta\alpha_{ij}\alpha_{ij}\frac{4}{3}\pi b^3 = \alpha_{ij}\int_S\left[\eta_0\left(\frac{\partial u_i^0}{\partial x_k}+\frac{\partial u_k^0}{\partial x_i}\right) - P'\delta_{ik} + \eta_0\left(\frac{\partial u_i'}{\partial x_k}+\frac{\partial u_k'}{\partial x_i}\right)\right]x_j n_k \, dS \quad (76)$$

Adding and subtracting the following surface integral

$$\alpha_{ij}\eta_0\int_S(u_i n_j + u_j n_i)\, dS \quad (77)$$

to the above-referred dissipation term, we have

$$2\eta\alpha_{ij}\alpha_{ij}\frac{4}{3}\pi b^3 = \int_S \alpha_{ij}\eta_0(u_i n_j + u_j n_i)\, dS + \int_S \alpha_{ij}\left\{\left[-P'\delta_{ik} + \eta_0\left(\frac{\partial u_i}{\partial x_k}+\frac{\partial u_k}{\partial x_i}\right)\right]x_j n_k - \eta_0(u_i n_j + u_j n_i)\right\} dS \quad (78)$$

Until this point, the formalism is the same as that shown in a previous paper,[2] where overlapping was not considered. For overlapping conditions, the perturbation pressure function takes the form

$$P'(\mathbf{r}) = -\eta_0\left(\frac{1}{2}\frac{d^3F}{dr^3}+\frac{3}{r}\frac{d^2F}{dr^2}+\frac{1}{r^2}\frac{\rho_{el}^0(r)\,\psi(r)}{\eta_0}\right)(\mathbf{r}\cdot\alpha\cdot\mathbf{r})$$

(see Appendix 2 for its derivation). Substituting this expression and the velocity field $\mathbf{u} = \alpha\cdot\mathbf{r}$ at the outer surface of the cell in eq 78, which is the above-mentioned Simha condition, we obtain

$$2\eta\ \mathrm{tr}(\alpha^2)\frac{4}{3}\pi b^3 = 2\eta_0\ \mathrm{tr}(\alpha^2)\frac{4}{3}\pi b^3 + 4\pi C_{N+1}2\eta_0\mathrm{tr}(\alpha^2) - 2\eta_0\ \mathrm{tr}(\alpha^2)\frac{D\phi}{5}\frac{4}{3}\pi b^3 \quad (79)$$

where D is expressed by

$$D = -\frac{\psi(b)}{\phi\eta_0}\rho_{el}^0(b) = -\frac{\psi(b)}{\phi\eta_0}\sum_{i=1}^{N} z_i e n_i^{\infty}\exp\left[-\frac{z_i e}{k_B T}\Psi^0(b)\right] \quad (80)$$

From eq 79 we obtain

$$\eta = \eta_0\left[1+\phi\left(\frac{3C_{N+2}}{a^3}-\frac{D}{5}\right)\right] \quad (81)$$

When the particles are uncharged, the asymptotic forms for the far-field behavior of the functions are indeed exact up to the surface of the particles. For the $F(r)$ function, this means that the expression (66) is exact and has to fulfill the boundary conditions (37) at the surface of the particle. The values of the unknown independent constants C_{N+2} and C_{N+3} can then be obtained. The effective viscosity for the uncharged case turns out to be

$$\eta = \eta_0\left[1+\frac{5}{2}\phi\left\{\frac{4(1-\phi^{7/3})}{4(1+\phi^{10/3})-25\phi(1+\phi^{4/3})+42\phi^{5/3}}\right\}\right] \quad (82)$$

or defining $S(\phi)$ (first derived by Simha) as

$$S(\phi) = \frac{4(1-\phi^{7/3})}{4(1+\phi^{10/3})-25\phi(1+\phi^{4/3})+42\phi^{5/3}} \quad (83)$$

the effective viscosity becomes

$$\eta = \eta_0\left[1+\frac{5}{2}\phi S(\phi)\right] \quad (84)$$

When the suspension is very dilute ($\phi \to 0$), the Simha function $S(\phi)$ tends to 1, and eq 84 transforms into Einstein result, as expected.

Electroviscous Coefficient. If the particles are charged, we can define an electroviscous coefficient p by analogy with the dilute case,

$$\eta = \eta_0\left[1+\frac{5}{2}\phi S(\phi)(1+p)\right] \quad (85)$$

Using eq 81, the electroviscous coefficient is given by

$$p = \frac{2}{5S(\phi)}\left(3\frac{C_{N+2}}{a^3}-\frac{D}{5}\right)-1 \quad (86)$$

In the limit of a very dilute suspension $\phi \to 0$, it is verified that

$$\lim_{\phi\to 0} S(\phi) = 1, \qquad \lim_{\phi\to 0} D = 0 \quad (87)$$

and the electroviscous coefficient tends to that calculated by Watterson and White.[16]

If the charge on the particles is zero ($\zeta = 0$), we have

$$C_{N+2}^{\zeta=0} = \frac{5a^3}{6} \quad (88)$$

and the electroviscous coefficient vanishes as expected.

In Figures 2−4, the influence of overlapping can be observed when the volume fraction is varied at constant electrokinetic radius, with values $\kappa a = 1$, $\kappa a = 10$ and $\kappa a = 25$, respectively. Symbols are plotted in all curves to distinguish between them clearly, although they are not experimental curves. In the first case ($\kappa a = 1$), the ionic diffuse layer thickness is high and the overlapping effect is important at any volume fraction in the figure. For $\kappa a = 10$, a high volume fraction ($\phi > 0.2$) is required to appreciate this effect because the diffuse layer thickness is relatively small, and for $\kappa a = 25$, only in the $\phi = 0.5$ case are differences appreciated. The data used in the generation of all figures can be found in Table 1. The drag coefficients λ_i in eq 10 are related to the limiting equivalent conductance Λ_i^0 of i-type ions by

$$\lambda_i = \frac{N_A e^2 |z_i|}{\Lambda_i^0} \quad (89)$$

where N_A is Avogadro's constant.

The dependence of the electroviscous coefficient against the variation of ϕ in Figures 2−4 presents very interesting features. In the case $\kappa a = 1$ (Figure 2), when the volume fraction is increased, the electroviscous coefficient diminishes. For $\kappa a =$

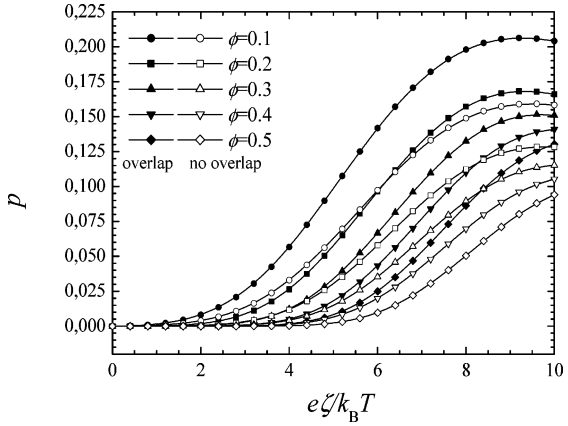

Figure 2. Electroviscous coefficient against dimensionless ζ-potential at $\kappa a = 1$ for various ϕ values.

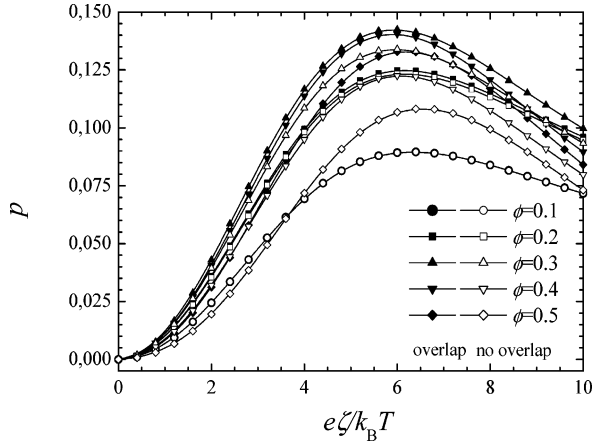

Figure 3. Electroviscous coefficient against dimensionless ζ-potential at $\kappa a = 10$ for various ϕ values.

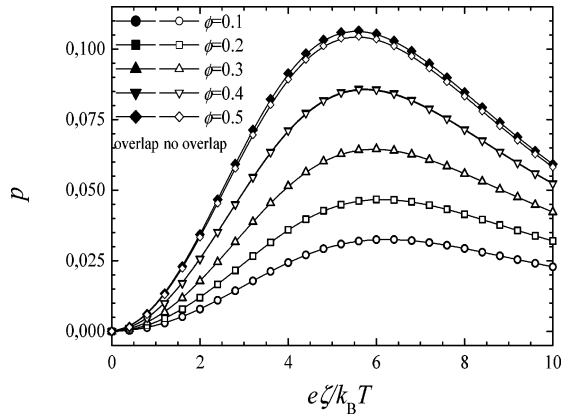

Figure 4. Electroviscous coefficient against dimensionless ζ-potential at $\kappa a = 25$ for various ϕ values.

25 (Figure 4), the dependence is the opposite: an increase of the volume fraction gives an increase of the electroviscous coefficient. For intermediate κa values, i.e., $\kappa a = 10$ (Figure 3), the electroviscous coefficient increases when ϕ changes from 0.1 to 0.3 and decreases afterward when ϕ increases until 0.5.

The reason for this behavior has to be found in the relative sizes of the electrical double layer and the cell. For low κa values, the diffuse layer is comparable or greater than the fluid shell inside the cell for all ϕ values presented (Figure 2), and an increase of the volume fraction sets the boundary conditions at the cell surface nearer to the particle surface, confining the double layer in a smaller region than it would have in the infinite diluted case for the same κa value. As a consequence, the

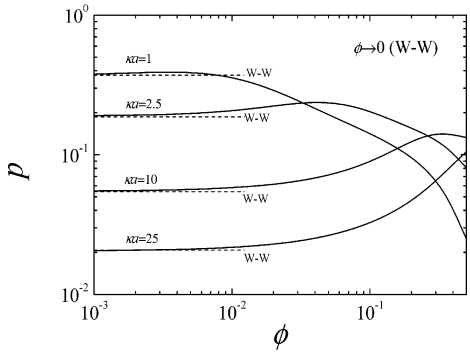

Figure 5. Electroviscous coefficient dependence with ϕ at constant ζ-potential ($e\zeta/k_BT = 6$) and various κa values. W−W is the Watterson−White's[16] limit for very dilute suspensions.

TABLE 1: Data Used in the Generation of the Figures

particle radius	$a = 100$ nm
temperature	$T = 298.16$ K
rel permittivity of suspending liquid	$\epsilon_{rs} = 78.55$
rel permittivity of solid particles	$\epsilon_{rp} = 2$
electrolyte	KCl
co-ion K^+ limiting equiv conductance	$\Lambda_-^0 = 76.31$ cm²/(ohm·g.equiv)
counterion Cl^- limiting equiv conductance	$\Lambda_-^0 = 73.48$ cm²/(ohm·g.equiv)

growing electrical body force acting inside the electrical double layer reduces its distortion, resulting in a diminution of energy dissipation and, consequently, of the electroviscous coefficient p.

On the contrary, for high κa values the double layer thickness is lower than the particle−cell surface distance for all ϕ values in Figure 4. The electroviscous coefficient rises with ϕ because the velocity gradients inside the electrical double layer augment when the cell radius decreases, without contracting the diffuse layer. The enhancement of the velocity gradients involves an increase of the distortion of the double layer.

Finally, at intermediate κa values, there is a competition between both mechanisms described above, which explains the observed p-maximum against ϕ in Figure 3.

In Figure 5 it is shown the electroviscous coefficient against the volume fraction at different values of the electrokinetic radius κa and constant dimensionless ζ-potential $e\zeta/k_BT = 6$. In this figure we see more clearly the ϕ dependence explained before: for all κa values there is a maximum of the electroviscous coefficient against the volume fraction. The maximum appears at a lower ϕ value when the electrokinetic radius is diminished.

The horizontal dashed lines indicate the results of Watterson and White[16] (W−W). These results are reproduced by our model in the limit of very dilute suspensions, as stated above.

In Figure 6 the dependence of p with κa and $e\zeta/k_BT$ is presented at a constant volume fraction $\phi = 0.01$. The volume fraction is low and at high κa values the results match those of Watterson and White.[16] However, at low κa values and high ζ potential the electroviscous coefficient is larger than those of Watterson and White due to the overlapping of adjacent ionic layers. This is better shown in Figure 7, where p is calculated both taking into account the overlapping and neglecting it ($D = 0$ in eq 86). Only for $\kappa a = 1$ do differences appear due to overlapping.

In Figure 8 the volume fraction is far from the dilute limit. The effect of particle concentration is now noticeable and we cannot compare with earlier results. It can be seen that the electroviscous coefficient has a remarkable maximum for all

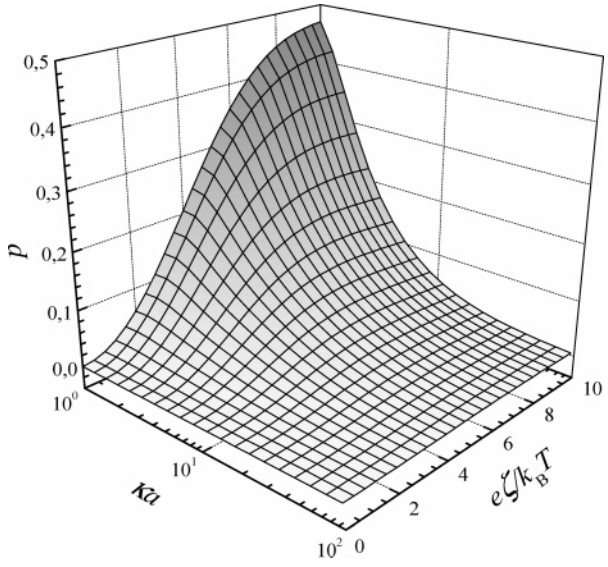

Figure 6. Electroviscous coefficient against κa and dimensionless ζ-potential for constant volume fraction $\phi = 0.01$.

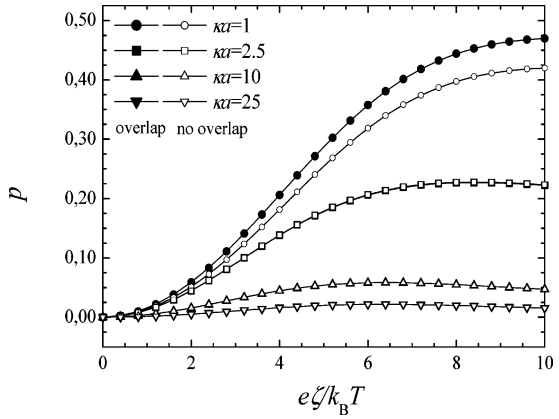

Figure 7. Electroviscous coefficient against dimensionless ζ-potential for constant volume fraction $\phi = 0.01$.

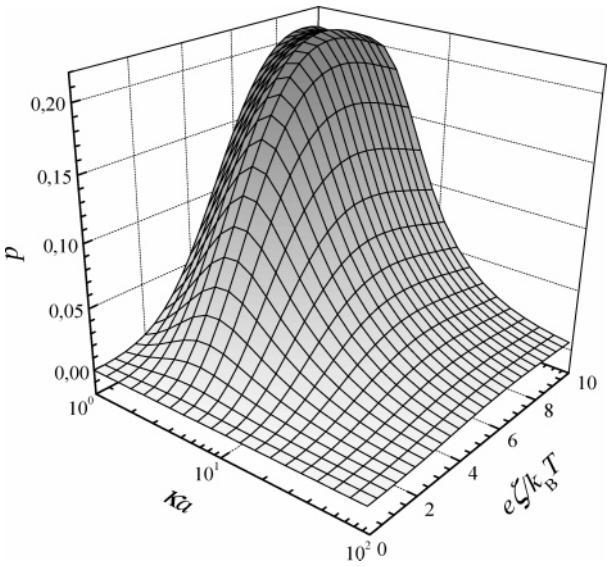

Figure 8. Electroviscous coefficient against κa and dimensionless ζ-potential for constant volume fraction $\phi = 0.1$.

κa and dimensionless ζ-potential values. It is usual to find a maximum of the primary electroviscous coefficient (i.e., in the very dilute limit of Watterson and White[16]) as a function of ζ-potential. Our interpretation of the maximum against ζ-potential is as follows: the dissipation of energy (and, consequently, the viscosity) increases with ζ when the potential is low because there are more ions in the double layer and the distortion of the flow field around the particles is higher. But if the potential rises sufficiently, the electrical body forces acting on the fluid inside the double layer reduces the distortion of the latter and tends to recover the equilibrium distribution. This means that the region of flow distortion is smaller and the system approaches the Einstein problem with an effective particle radius larger than the true radius of the solid particles.

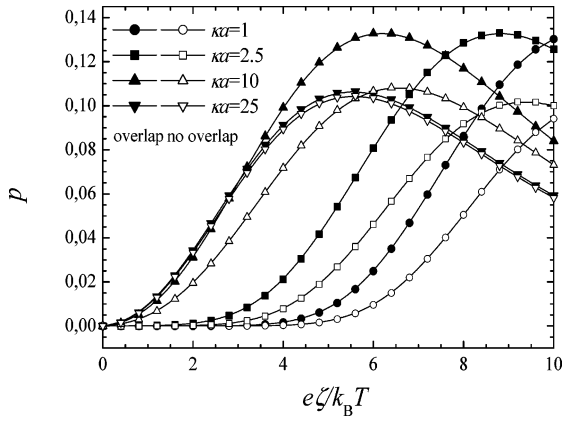

Figure 9. Electroviscous coefficient against dimensionless ζ-potential at $\phi = 0.5$ for various κa values.

The maximum of p against the electrokinetic radius κa is due to the overlapping of adjacent ionic layers and, therefore, has not any analogue in the model of Watterson and White.[16] The physical interpretation is that, as the electrokinetic radius decreases, the Debye length is greater and the region of double layer distortion increases, leading to more energy dissipation. On the other hand, the number density of ions inside the diffuse layer is also decreasing and this contributes to a lower viscosity. The competition between them explains the maximum.

Finally, in Figure 9, we show the calculations of the electroviscous coefficient for a volume fraction close to the limit of what, we believe, is the limit of validity of the model ($\phi = 0.5$). In this case the cell is very small; therefore, κa must be very high for the effect of overlapping to disappear. The maximum in p occurs at lower ζ-potential as κa increases. This means that, as the ionic diffuse layer is smaller, the effect of the electrical body force in it, which makes it less deformable, happens at lower potentials (according to the interpretations given above).

But the most remarkable feature on this graph is the increase of p as κa increases up to $\kappa a = 10$ and the following decrease at $\kappa a = 25$. The reason for this curious behavior is that we are at very high particle concentration, leading to a very small cell size (the conditions for no perturbation are imposed close to the particle surface). When the Debye length increases ($\kappa a = 25 \rightarrow \kappa a = 10$) the ionic diffuse layer grows up inside the cell and, then, the distorted region is bigger. Nevertheless, when this layer is larger than the cell, what one gets when κa decreases is that the number of ions inside the cell is decreasing and, consequently, the dissipated energy is smaller.

It can be observed in Figures 2−4, 7, and 9 presented above that when the contribution of the overlapping of adjacent ionic double layers is included in the theoretical model (overlap curves), the electroviscous coefficient is higher than in the case it is not taken into account (no-overlap curves).

It also follows from the precedent discussions that generally the electroviscous coefficient diminishes when the electrokinetic

radius is increased and rises with particle volume fraction and ζ potential. This assertion is always true provided that the phenomenon of "rigidization" of the electrical double layer does not appear. The appearance of "rigidization" occurs if the particle volume fraction and/or the ζ-potential are augmented at constant electrokinetic radius. In Figures 5 and 8 it can be observed that the bigger the electrical double layer (i.e., the smaller the electrokinetic radius), the lower the ϕ value or the higher the ζ-potential value where the phenomenon takes place.

We think that the model presented in this work can improve the agreement between theory and experiment in the primary electroviscous effect. As mentioned in the Introduction, there is an underestimation of the effect by the theoretical models, especially under conditions of very low ionic concentrations. In its experimental determination, it is usual to reach ϕ values of the order of $\phi = 0.01$. This means that, for colloidal particles of 100 nm radius and a 1:1 electrolyte concentration 10^{-5} M, the particle−cell surface distance $(b - a)$ is about only 3.7 times the double layer thickness κ^{-1} in that case, and for a 2:1 electrolyte concentration 10^{-6} M, we find that $(b - a) \approx 2.05\kappa^{-1}$. As we can infer from these examples, there must be some influence of the hydrodynamic interactions and overlapping of adjacent diffuse layers that is not being taken into account.

In addition, with a new theoretical model able to predict the electroviscous coefficient of moderately concentrated suspensions, it is possible to extend the range of ϕ values in the experimental studies of the electroviscous effect, making the comparison theory−experiment more reliable and easier to get than in the dilute limit. We stress the necessity of new experimental works to check the validity of the present theory. A Fortran program for the calculation of the electroviscous effect is available from the authors.

Appendix 1: Boundary Condition for the Function $\psi(r)$ at the Particle Surface

By substituting the expressions

$$\delta\Psi(\mathbf{r}) = \psi(r)(\hat{\mathbf{r}}\cdot\alpha\cdot\hat{\mathbf{r}}) \tag{90}$$

$$\delta\Psi_p(\mathbf{r}) = \psi_p(r)(\hat{\mathbf{r}}\cdot\alpha\cdot\hat{\mathbf{r}}) \tag{91}$$

in the boundary condition (35), we obtain

$$\epsilon_{rs}[\hat{\mathbf{r}}\cdot\nabla(\psi(r)(\hat{\mathbf{r}}\cdot\alpha\cdot\hat{\mathbf{r}}))]|_{r=a} = \epsilon_{rp}[\hat{\mathbf{r}}\cdot\nabla(\psi_p(r)(\hat{\mathbf{r}}\cdot\alpha\cdot\hat{\mathbf{r}}))]|_{r=a} \tag{92}$$

Operating in this equality, we have

$$\epsilon_{rs}\frac{d\psi}{dr}(a) = \epsilon_{rp}\frac{d\psi_p}{dr}(a) \tag{93}$$

We need an expression for the derivative in the second member of eq 93.

The Laplace equation for the electric potential inside the particle must be satisfied, so

$$\nabla^2\delta\Psi_p(\mathbf{r}) = 0 \tag{94}$$

By substituting expression (91) in this equation, we obtain the equation for the function $\psi_p(r)$,

$$L_2\psi_p(r) = \frac{d^2\psi_p(r)}{dr^2} + \frac{2}{r}\frac{d\psi_p(r)}{dr} - \frac{6}{r^2}\psi_p(r) = 0 \tag{95}$$

The general solution of this equation is

$$\psi_p(r) = C_1 r^2 + C_2\frac{1}{r^3} \tag{96}$$

The constant C_2 must be zero because $\delta\Psi_p(\mathbf{r})$ has to be finite for $r \le a$, and then $\psi_p(r) = C_1 r^2$.

According to the boundary condition (34),

$$\delta\Psi(r)|_{r=a} = \delta\Psi_p(r)|_{r=a} \tag{97}$$

and substituting the latter result, we obtain

$$C_1 r^2(\hat{\mathbf{r}}\cdot\alpha\cdot\hat{\mathbf{r}})|_{r=a} = \psi(r)(\hat{\mathbf{r}}\cdot\alpha\cdot\hat{\mathbf{r}})|_{r=a} \tag{98}$$

and then

$$C_1 = \frac{\psi(a)}{a^2} \tag{99}$$

The radial perturbation in the interior electrical potential is, finally,

$$\psi_p(r) = \frac{\psi(a)}{a^2}r^2 \tag{100}$$

Operating with the latter potential function in eq 93, the boundary condition (42) for the perturbation potential at the particle surface is obtained

$$\epsilon_{rs}\frac{d\psi}{dr}(a) = \epsilon_{rp}\frac{2\psi(a)}{a} \Rightarrow \frac{d\psi}{dr}(a) - \frac{2\epsilon_{rp}}{\epsilon_{rs}}\frac{\psi(a)}{a} = 0 \tag{101}$$

Appendix 2. Perturbation Pressure Function

We need a full solution for the perturbation pressure function of the Navier−Stokes equation

$$\eta_0\nabla^2\mathbf{u}(\mathbf{r}) - \nabla P(\mathbf{r}) = \rho_{el}(\mathbf{r})\nabla\Psi(\mathbf{r}) \tag{102}$$

Substituting the following perturbed quantities

$$n_i(\mathbf{r}) = n_i^0(r) + \delta n_i(\mathbf{r}) \qquad i=1, ..., N \tag{103}$$

$$P(\mathbf{r}) = P^0(r) + P'(\mathbf{r}) \qquad \Psi(\mathbf{r}) = \Psi^0(r) + \delta\Psi(\mathbf{r}) \tag{104}$$

$$\rho_{el}(\mathbf{r}) = \rho_{el}^0(r) + \delta\rho_{el}(\mathbf{r}) \qquad \delta\rho_{el}(\mathbf{r}) = \sum_{i=1}^{N} z_i e\delta n_i(\mathbf{r}) \tag{105}$$

$$\delta n_i(\mathbf{r}) = -\left(\frac{z_i e}{k_B T}\right)n_i^0(r)[\delta\Psi(\mathbf{r}) + \Phi_i(\mathbf{r})] = -\left(\frac{z_i e}{k_B T}\right)n_i^0(r)[\psi(r) + \phi_i(r)](\hat{\mathbf{r}}\cdot\alpha\cdot\hat{\mathbf{r}}) \tag{106}$$

in the Navier−Stokes equation (102) yields

$$\nabla P^0(r) + \nabla P'(\mathbf{r}) = -\eta_0\nabla\times\nabla\times\mathbf{u}(\mathbf{r}) - \rho_{el}(\mathbf{r})\nabla\Psi(\mathbf{r}) = -\eta_0\nabla\times\nabla\times\mathbf{u}(\mathbf{r}) - \rho_{el}^0(r)\nabla\Psi^0(r) - \rho_{el}^0(r)\nabla\delta\Psi(\mathbf{r}) - \delta\rho_{el}(\mathbf{r})\nabla\Psi^0(r) - \delta\rho_{el}(\mathbf{r})\nabla\delta\Psi(\mathbf{r}) \tag{107}$$

In equilibrium conditions the equation

$$\nabla P^0(r) = -\rho_{el}^0(r)\,\nabla\Psi^0(r) \tag{108}$$

is satisfied and the corresponding terms in eq 107 are canceled. In addition, the last nonlinear term in eq 107 can be eliminated

because we are looking for the linear response in α, i.e.,

$$\delta\rho_{el}(\mathbf{r}) = \sum_{i=1}^{N} z_i e \delta n_i(\mathbf{r}) = -\sum_{i=1}^{N}\left(\frac{z_i^2 e^2}{k_B T}\right) n_i^0(r)[\psi(r) + \phi_i(r)](\hat{\mathbf{r}}\cdot\alpha\cdot\hat{\mathbf{r}}) = t(r)(\hat{\mathbf{r}}\cdot\alpha\cdot\hat{\mathbf{r}}) \quad (109)$$

$$\nabla\delta\Psi(\mathbf{r}) = \nabla[\psi(r)(\hat{\mathbf{r}}\cdot\alpha\cdot\hat{\mathbf{r}})] = \nabla\left[\frac{\psi(r)}{r^2}(\mathbf{r}\cdot\alpha\cdot\mathbf{r})\right] = \nabla\left[\frac{\psi(r)}{r^2}\right](\mathbf{r}\cdot\alpha\cdot\mathbf{r}) + \frac{\psi(r)}{r^2}\nabla(\mathbf{r}\cdot\alpha\cdot\mathbf{r}) = r^2\frac{d}{dr}\left[\frac{\psi(r)}{r^2}\right]\hat{\mathbf{r}}(\hat{\mathbf{r}}\cdot\alpha\cdot\hat{\mathbf{r}}) + \frac{\psi(r)}{r}2(\alpha\cdot\hat{\mathbf{r}}) \quad (110)$$

$$\delta\rho_{el}(\mathbf{r})\nabla\delta\Psi(\mathbf{r}) = [t(r)(\hat{\mathbf{r}}\cdot\alpha\cdot\hat{\mathbf{r}})]\left\{r^2\frac{d}{dr}\left[\frac{\psi(r)}{r^2}\right]\hat{\mathbf{r}}(\hat{\mathbf{r}}\cdot\alpha\cdot\hat{\mathbf{r}}) + \frac{\psi(r)}{r}2(\alpha\cdot\hat{\mathbf{r}})\right\} \approx O(\alpha^2) \quad (111)$$

the function $t(r)$ being defined in eq 109.

Simplifying and rearranging terms, we obtain

$$\nabla P'(\mathbf{r}) = -\eta_0\nabla\times\nabla\times\mathbf{u}(\mathbf{r}) - \rho_{el}^0(r)\nabla\delta\Psi(\mathbf{r}) - \delta\rho_{el}(\mathbf{r})\nabla\Psi^0(r) = -\eta_0\nabla\times\nabla\times\mathbf{u}(\mathbf{r}) - \rho_{el}^0(r)r^2\frac{d}{dr}\left[\frac{\psi(r)}{r^2}\right]\hat{\mathbf{r}}(\hat{\mathbf{r}}\cdot\alpha\cdot\hat{\mathbf{r}}) - \rho_{el}^0(r)\frac{2\psi(r)}{r}(\alpha\cdot\hat{\mathbf{r}}) - t(r)\left(\frac{d\Psi^0(r)}{dr}\right)\hat{\mathbf{r}}(\hat{\mathbf{r}}\cdot\alpha\cdot\hat{\mathbf{r}}) \quad (112)$$

As the velocity field from eqs 5 and 25 can be expressed by

$$\mathbf{u}(\mathbf{r}) = (\alpha\cdot\hat{\mathbf{r}})\left[r - 3F(r) - r^2\frac{d}{dr}\left(\frac{F(r)}{r}\right)\right] + r^2\frac{d}{dr}\left(\frac{F(r)}{r}\right)\hat{\mathbf{r}}(\hat{\mathbf{r}}\cdot\alpha\cdot\hat{\mathbf{r}}) \quad (113)$$

operating, we obtain

$$\nabla\times\nabla\times\mathbf{u}(\mathbf{r}) = r^2\frac{dg(r)}{dr}\hat{\mathbf{r}}(\hat{\mathbf{r}}\cdot\alpha\cdot\hat{\mathbf{r}}) - \left[r^2\frac{dg(r)}{dr} + 3rg(r)\right](\alpha\cdot\hat{\mathbf{r}}) \quad (114)$$

where the function $g(r)$ is given by

$$g(r) = -\frac{1}{r}\frac{d^2F(r)}{dr^2} - \frac{4}{r^2}\frac{dF(r)}{dr} + 4\frac{F(r)}{r^3} \quad (115)$$

Substituting the latter results in the linearized Navier−Stokes equation (112) for the perturbation pressure yields, after rearranging terms, yields

$$\nabla P'(\mathbf{r}) = \left\{-\eta_0 r^2\frac{dg(r)}{dr} - \rho_{el}^0(r)r^2\frac{d}{dr}\left[\frac{\psi(r)}{r^2}\right] - t(r)\left(\frac{d\Psi^0(r)}{dr}\right)\right\}\hat{\mathbf{r}}(\hat{\mathbf{r}}\cdot\alpha\cdot\hat{\mathbf{r}}) + \left\{\eta_0\left[r^2\frac{dg(r)}{dr} + 3rg(r)\right] - \rho_{el}^0(r)\frac{2\psi(r)}{r}\right\}(\alpha\cdot\hat{\mathbf{r}}) \quad (116)$$

On the other hand, symmetry conditions permit us to express the perturbation pressure function as

$$P'(\mathbf{r}) = h(r)(\hat{\mathbf{r}}\cdot\alpha\cdot\hat{\mathbf{r}}) \quad (117)$$

and then, its gradient turns out to be

$$\nabla P'(\mathbf{r}) = \left[r^2\frac{d}{dr}\left(\frac{h(r)}{r^2}\right)\right]\hat{\mathbf{r}}(\hat{\mathbf{r}}\cdot\alpha\cdot\hat{\mathbf{r}}) + \left[\frac{2h(r)}{r}\right](\alpha\cdot\hat{\mathbf{r}}) \quad (118)$$

Equating the terms with the same vector dependences in the two expressions (116) and (118), we obtain the following two equations

$$\left[r^2\frac{d}{dr}\left(\frac{h(r)}{r^2}\right)\right] = -\eta_0 r^2\frac{dg(r)}{dr} - \rho_{el}^0(r)r^2\frac{d}{dr}\left[\frac{\psi(r)}{r^2}\right] - t(r)\left(\frac{d\Psi^0(r)}{dr}\right) \quad (119)$$

$$\left[\frac{2h(r)}{r}\right] = \eta_0\left[r^2\frac{dg(r)}{dr} + 3rg(r)\right] - \rho_{el}^0(r)\frac{2\psi(r)}{r} \quad (120)$$

The $h(r)$ function, and then, the pressure function, can be derived from the second one

$$P'(\mathbf{r}) = \left\{\eta_0\left[\frac{r^3}{2}\frac{dg(r)}{dr} + \frac{3r^2}{2}g(r)\right] - \rho_{el}^0(r)\,\psi(r)\right\}(\hat{\mathbf{r}}\cdot\alpha\cdot\hat{\mathbf{r}}) \quad (121)$$

Replacing now the function $g(r)$ and its first derivative in the latter equation, we finally obtain

$$P'(\mathbf{r}) = -\eta_0\left\{\frac{r^2}{2}\frac{d^3F}{dr^3} + 3r\frac{d^2F}{dr^2} + \frac{\rho_{el}^0(r)\,\psi(r)}{\eta_0}\right\}(\hat{\mathbf{r}}\cdot\alpha\cdot\hat{\mathbf{r}}) \quad (122)$$

We now have to check that eq 119 is satisfied for the $h(r)$ function we have just calculated. Replacing $h(r)$ in the first member of eq 119 and substituting the $t(r)$ function and the first derivative of the $g(r)$ function in the second member we obtain, after rearranging terms,

$$\frac{d^4F(r)}{dr^4} + \frac{8}{r}\frac{d^3F(r)}{dr^3} - \frac{24}{r^3}\frac{dF(r)}{dr} + \frac{24F(r)}{r^4} = -\frac{2e^2}{r^2\eta_0 k_B T}\left(\frac{d\Psi^0(r)}{dr}\right)\sum_{i=1}^{N} z_i^2 n_i^0(r)\,\phi_i(r) \quad (123)$$

which is the differential eq 22 satisfied by the $F(r)$ function.

Acknowledgment. Financial support for this work by Ministerio de Ciencia y Tecnología, Spain (Project MAT2003-04688) is gratefully acknowledged by E. Ruiz-Reina and F. Carrique.

References and Notes

(1) Einstein, A. *Ann. Phys.* **1906**, *19*, 289; **1911**, *34*, 591.
(2) Ruiz-Reina, E.; Carrique, F.; Rubio-Hernández, F.J.; Gómez-Merino, A. I.; García-Sánchez, P. *J. Phys. Chem B* **2003**, *107*, 9528.
(3) García-Salinas, M. J.; de las Nieves, F. J. *Colloids Surf. A* **2003**, 222, 65.
(4) Stone-Masui, J.; Watillon, A. *J. Colloid Interface Sci.* **1968**, *28*, 187.
(5) Honig, E. P.; Pünt, W. F. J.; Offermans, P. H. G. *J. Colloid Interface Sci.* **1990**, *134*, 169.
(6) McDonough, R. W.; Hunter, R. J. *J. Rheol.* **1983**, *27*, 189.
(7) Delgado, A. V.; González-Caballero, F.; Cabrerizo, M. A.; Alados, I. *Acta Polym.* **1987**, *38*, 66.
(8) Zurita, L.; Carrique, F.; Delgado, A. V. *Colloids Surf. A* **1994**, *92*, 23.
(9) Rubio-Hernández, F. J.; Gómez-Merino, A. I.; Ruiz-Reina, E.; Carnero-Ruiz, C. *Colloids Surf. A* **1998**, *140*, 295.
(10) Ali, S. A.; Sengupta, M. *J. Colloid Interface Sci.* **1998**, *204*, 219.
(11) Rubio-Hernández, F. J.; Ruiz-Reina, E.; Gómez-Merino, A. I. *Colloids Surf. A* **1999**, *159*, 373.

(12) Smoluchowski, M. *Kolloid Z.* **1916**, *18*, 194.
(13) Booth, F. *Proc. R. Soc. A* **1950**, *203*, 533.
(14) Russel, W. B. *J. Fluid Mech.* **1978**, *85*, 673.
(15) Sherwood, J. D. *J. Fluid Mech.* **1980**, *101*, 609.
(16) Watterson, I. G.; White, L. R. *J. Chem. Soc., Faraday Trans. 2* **1981**, *77*, 1115.
(17) Hinch, E. J.; Sherwood, J. D. *J. Fluid Mech.* **1983**, *132*, 337.
(18) Rubio-Hernández, F. J.; Ruiz-Reina, E.; Gómez-Merino, A. I. *J. Colloid Interface Sci.* **1998**, *206*, 334.
(19) Rubio-Hernández, F. J.; Ruiz-Reina, E.; Gómez-Merino, A. I. *J. Colloid Interface Sci.* **2000**, *226*, 180.
(20) Rubio-Hernández, F. J.; Ruiz-Reina, E.; Gómez-Merino A. I.; Sherwood, J. D. *Rheol. Acta* **2001**, *40*, 230.
(21) Rubio-Hernández, F. J.; Ruiz-Reina, E.; Gómez-Merino, A. I. *Colloids Surf. A* **2001**, *192*, 349.
(22) Sherwood, J. D.; Rubio-Hernández F. J.; Ruiz-Reina, E. *J. Colloid Interface Sci.* **2000**, *228*, 7.
(23) Happel, J. *J. Appl. Phys.* **1957**, *28*, 1288.
(24) Simha, R. *J. Appl. Phys.* **1952**, *23*, 1020.
(25) Landau, L. D.; Lifshitz, E. M. *Fluid Mechanics*, 2nd ed.; Butterworth-Heinemann: Oxford, U.K., 2000.
(26) DeLacey, E. H. B.; White, L. R. *J. Chem. Soc., Faraday Trans. 2* **1981**, *77*, 2007.
(27) Batchelor, G. K. *An Introduction to Fluid Dynamics*; Cambridge University Press: Cambridge, U.K., 1967.
(28) Levine, S.; Neale, G. H. *J. Colloid Interface Sci.* **1974**, *47*, 520.
(29) Ohshima, H. *J. Colloid Interface Sci.* **1999**, *212*, 443.
(30) Lee, E.; Chih, M. H.; Hsu, J. P. *J. Phys. Chem B* **2001**, *105*, 747.
(31) Carrique, F.; Arroyo, F. J.; Delgado, A. V. *J. Colloid Interface Sci.* **2002**, *252*, 126.
(32) Levine, S.; Neale, G. H.; Epstein, N. *J. Colloid Interface Sci.* **1976**, *57*, 424.
(33) Ohshima, H. *J. Colloid Interface Sci.* **1998**, *208*, 295.
(34) Ohshima, H. *J. Colloid Interface Sci.* **1997**, *195*, 137.
(35) Lee, E.; Yen, F. Y.; Hsu, J. P. *J. Phys. Chem B* **2001**, *105*, 7239.
(36) Hsu, J. P.; Lee, E.; Yen, F. Y. *J. Phys. Chem B* **2002**, *106*, 4789.
(37) Carrique, F.; Arroyo, F. J.; Jiménez, M. L.; Delgado, A. V. *J. Chem. Phys.* **2003**, *118*, 1945
(38) Ohshima, H.; Dukhin, A. S. *J. Colloid Interface Sci.* **1999**, *212*, 449.
(39) Dukhin, A. S.; Ohshima, H.; Shilov, V. N.; Goetz, P. J. *Langmuir* **1999**, *15*, 3445.
(40) Macosko, C. W. *Rheology: Principles, Measurements and Applications*; John Wiley & Sons: New York, U.S.A., 1994.